Modelling ultrafast magnetization dynamics in 2D van der Waals material $Cr_2Ge_2Te_6$

Theodor Griepe and Unai Atxitia*
Instituto de Ciencia de Materiales de Madrid, CSIC, Cantoblanco, 28049 Madrid, Spain
(Dated: October 25, 2022)

We investigate the ultrafast magnetization dynamics induced by femtosecond laser pulses in $Cr_2Ge_2Te_6$. In particular, we study the origin of the fluence dependence of the magnetization dynamics in $Cr_2Ge_2Te_6$ in a large range of time scales, from sub-picosecond to nanoseconds. The dependence on the initial temperature is also investigated. Our study involves the numerical solution of the equation of motion for the magnetization and the so-called two temperature model, which calculates the evolution of the electron and phonon temperatures.

MICROSCOPIC THREE TEMPERATURE MODEL

The microscopic three temperature model (MT3M) describes ultrafast magnetization dynamics by the intrinsic mechanism of electron-phonon-mediated spin flips [2]. As such, the model describes the energy of internally thermalized electron and lattice systems through their respective temperatures T_e and T_p as well as their corresponding specific heats C_e and C_p. The M3TM assumes that the spin system is not internally thermalized so that the magnetization dynamics cannot be described by a temperature. Instead, the magnetization dynamics are described microscopically by spin-flips upon an electron-phonon scattering event. These microscopic processes led to a net magnetization dynamics which can be described by the combination of the two-temperature model and an equation of motion for the non-equilibrium microscopic magnetization distribution.

Energy dynamics

The two-temperature model (2TM) is described by two coupled equations of motion for the electron and phonon temperatures:

$$C_\mathrm{e}\frac{dT_\mathrm{e}}{dt} = g_{\mathrm{e-p}}(T_\mathrm{p}-T_\mathrm{e}) + S(t) + \dot{Q}_\mathrm{es} \tag{1}$$

$$C_\mathrm{p}\frac{dT_\mathrm{p}}{dt} = -g_{\mathrm{e-p}}(T_\mathrm{p}-T_\mathrm{e}) \tag{2}$$

The absorbed laser pulse power is represented by a Gaussian function, $S(t)$. The electron heat capacity is $C_\mathrm{e} = \gamma_\mathrm{e} T_\mathrm{e}$. The electron-phonon coupling $g_{\mathrm{e-p}}$ allows for temperature equilibration of hot electrons and the lattice on the time scale determined by the ratio $g_{\mathrm{e-p}}/C_\mathrm{e}$. $\dot{Q}_{\mathrm{e-s}}$ defines the energy exchange between the spin and electron systems. An important aspect of the two temperature model in Eqs. (1) and (2) is the exact value of C_e, C_p, and $g_{\mathrm{e-p}}$. We take these parameters from experiments, which are summarized in Table 1. The subsystem specific energy (temperature) dynamics are captured in Eqs. (1) and (2).

The temporal evolution of the pump pulse is assumed to be of a Gaussian shape

$$S(t) = S_0 \exp\left\{-\frac{(t-t_0)^2}{2\sigma^2}\right\}, \tag{3}$$

centered around t_0 and duration σ. S_0 represents the energy density from the laser which is absorbed by the electron system. One can calculate the total absorbed-energy density as

$$E_\mathrm{pump} = \int_{-\infty}^{\infty} dt\ S(t) = \sqrt{2\pi} S_0 \sigma \tag{4}$$

$$\tag{5}$$

The absorbed energy by the electrons first heats the electron system up to relatively high temperatures. Once the laser pump of energy is gone this excess of energy is transferred to (i) the lattice by $g_{\mathrm{e-p}}(T_\mathrm{e}-T_\mathrm{p})$ and (ii) the spin system via

$$\dot{Q}_{\mathrm{e-s}} = Jm\dot{m}/V_{\mathrm{at}}, \tag{6}$$

where V_{at} denotes the mean atomic volume, calculated by dividing the unit cell volume by the number of atoms in a unit cell. The inclusion of Eq. (6) in the rate equation for the electron temperature allows for the conservation of the total energy in a non-equilibrium fashion, as electron and spin systems are not in equilibrium throughout the dynamical process. The exchange energy J is linked to the Curie temperature through the mean field approximation (MFA) by:

$$J = 3\frac{S^2}{S(S+1)}k_B T_C \tag{7}$$

The specific heat of the electron system is computed in the Sommerfeld (free electron model) approximation

$$C_{\mathrm{e}} = \gamma_{\mathrm{e}} T_{\mathrm{e}}, \tag{8}$$

where γ_{e} is the Sommerfeld coefficient and the lattice specific heat is computed with the Einstein model, where

$$C_{\mathrm{p}} = C_{\mathrm{p}\infty}\frac{T_{\mathrm{Ein}}^2}{T_{\mathrm{p}}^2}\frac{\exp\left\{\frac{T_{\mathrm{Ein}}}{T_{\mathrm{p}}}\right\}}{(\exp\left\{\frac{T_{\mathrm{Ein}}}{T_{\mathrm{p}}}\right\}-1)^2}. \tag{9}$$

For intermediate temperatures, the Debye model can be described by the Einstein model using the following relation between the Einstein temperature (T_{Ein}) and Debye temperature (T_{Debye}) approximately $T_{\mathrm{Ein}} = 0.75\ T_{\mathrm{Debye}}$. Thus, we use experimentally measured Debye temperature as a input for our model through that relation.

The electron-phonon coupling constant $g_{\mathrm{e-p}}$ is assumed to be independent of temperature. The value of the electron-phonon is critical for the adequate description of the temperature dynamics, which defines the shape of the magnetization dynamics in the first picoseconds. However, a definitive experimental value of $g_{\mathrm{e-p}}$ for CGT is still missing. By fitting our model to experimental results, we find a value for it. It is important to note that we have included a term into the rate equation for the electron temperature that describes the energy flow between the spin and electron system. Recently, it has been used in the simulation of the ultrafast energy flow in 3d transition metals but within an atomistic spin model[4].

Another important note is that we have assumed that the heating produced by the laser pulse is homogeneously distributed over the sample thickness. This approximation is justified due to the large penetration depth and small thermal conductivity between layers. Thus, effectively we only need to solve the equation of motion for one layer. We have tested the effect of thermal transport for realistic parameters and its effect is marginal.

Magnetization dynamics equations

The magnetization dynamics are described by the solution of Eqs. (10)-(12). This model is an extension of the M3TM (valid only for $S = 1/2$) for arbitrary values of the spin system S. This model has been recently derived by Beens et al. in Ref. [1]. For CGT we use $S = 3/2$.

The equation of motion for the magnetization dynamics requires the solution of three equations. The magnetization dynamics are determined by the statistical change of occupation numbers f_{m_s} of the S_z component m_s:

$$\frac{dm}{dt} = -\frac{1}{S}\sum_{ms=-S}^{ms=+S} m_s \frac{df_{m_s}}{dt} \tag{10}$$

$$\frac{df_{m_s}}{dt} = -(W^+_{m_s} + W^-_{m_s})f_{m_s} + W^+_{m_{s-1}} f_{m_{s-1}} + W^-_{m_{s+1}} f_{m_{s+1}} \tag{11}$$

$$W^\pm_{m_s} = R\frac{Jm}{4Sk_BT_c}\frac{T_p}{T_c}\frac{\mathrm{e}^{\mp\frac{Jm}{2Sk_BT_e}}}{\sinh(\frac{Jm}{2Sk_BT_e})}(S(S+1) - m_s(m_s \pm 1)) \tag{12}$$

The analytical description of the transition rates $W^\pm_{m_s}$ was introduced by Beens et al. [1]. The rate parameter R depends on the microscopic parameters of the system, and it is proportional to the spin-flip probability, a_{sf}.
The reduced total magnetization m is computed through the weighed sum of the occupations f_{m_s} of spin-z levels m_s. The dynamics of f_{m_s} are calculated from Eq. (11). The first term corresponds to the reduction of occupation through scattering into higher and lower neighbouring spin-levels. The second and third term correspond to an increase of the occupation due to scattering from (i) lower and (ii) higher spin levels, respectively. The rates $W^\pm_{m_s}$ are computed from applying Fermis golden rule to the Hamiltonian that describes a localized spin flip upon electron-phonon scattering, where a phonon either gets emitted ($a^\dagger_q$) or adsorbed (a_q):

$$\mathcal{H}_{\mathrm{eps}} = \sqrt{\frac{a_{sf}}{D_S}}\frac{\lambda_{ep}}{N^{3/2}}\sum_{k,k'}\sum_{q}^{ND_P}\sum_{j}^{N_S} c^\dagger_k c_{k'}(s_{j,+} + s_{j,-})(a^\dagger_q + a_q) \tag{13}$$

a_{sf} denotes the spin flip probability upon an electron-phonon scattering event. The rate parameter in equation (10) is then

$$R = 8\frac{a_{\mathrm{sf}} g_{\mathrm{e-p}} T_C^2 V_{\mathrm{at}}}{\mu_{\mathrm{at}} k_B T^2_{\mathrm{Debye}}}, \tag{14}$$

where μ_{at} is the atomic magnetic moment in units of the Bohr magneton and k_B is the Boltzmann constant.

Simulation setup; input parameters

The following Table shows the parameters we have used for the simulations (please add references for all the parameters):

Symbol	Description	Value	Units
γ_{e}	Sommerfeld constant	736.87	J/m^{3}K^2
$C_{p\infty}$	maximum lattice spec. heat	8.9×10^6	J/m^{3}K
$g_{\mathrm{e-p}}$	el.-ph. coupling	15×10^{16}	W/m^{3}K
T_C	Curie temp.	65[3]	K
T_{Debye}	Debye temp.	175 [3]	K
T_{Ein}	Einstein temp.	131	K
S	effective spin	3/2 [3]	/
μ_{at}	atom. magn. moment	4	μ_{B}
a_{sf}	spin-flip prob.	0.2	/
V_{at}	atomic volume	100	Å^3

With the above parameters the resulting rate parameter is $R = 0.06[\mathrm{ps}^{-1}]$. The resulting spin-flip probability $a_{\mathrm{sf}} = 0.2$ is a bit larger than in other materials $a_{\mathrm{sf}} = 0.05 - 0.1$. This value can be reduced by assuming a bit larger atomic volume. This will have a small effect on the dynamics.

Characterization of the pump pulse

For the pump pulse we have used the following parameters, where S_0 corresponds to the value used for the lowest fluence:

Symbol	Value	Units
σ	20	fs
S_0	10^{21}	W/m^3

The above parameters result in an absolute absorbed energy density of $E_{\text{pump}} = 50 \times 10^3$ mJ/cm^3. Assuming that the pump laser penetrates the sample along the c-axis with length $c = 2$ nm and uniform absorption of the pulse energy, we estimate the absorbed fluence through

$$\begin{aligned} F_a &= E_{\text{pump}}\ 2 \times 10^{-7}\text{cm} \\ &= 0.01 \frac{\text{mJ}}{\text{cm}^2} \end{aligned}$$

Fitting procedure

By comparison to the experimental results, we extracted the value of two parameters of the model, the electron-phonon coupling and the rate parameter. The other system parameters are assumed to be known and taken from literature. First, the electron-phonon coupling constant $g_{\text{e-p}}$ was taken as a fit parameter to match the timescale of the initial demagnetization phase occuring in the first 10 ps, as this timescale is defined by the equilibration time of the electron and phonon temperature. Second, the rate parameter R is adjusted by fitting the longer time scale magnetization dynamics, from 10 ps until magnetization equilibrium is reached for the highest fluence value. We then use this parameter R value for all the rest cases.

Simulation results; two-step demagnetization

The following Figures show the dynamics of the magnetization and electron/lattice temperatures for different fluences and different initial temperatures, respectively. Shown is the magnetization change $\Delta m = m(t) - m(t = 0)$, as this scales linearly in Kerr-rotation:

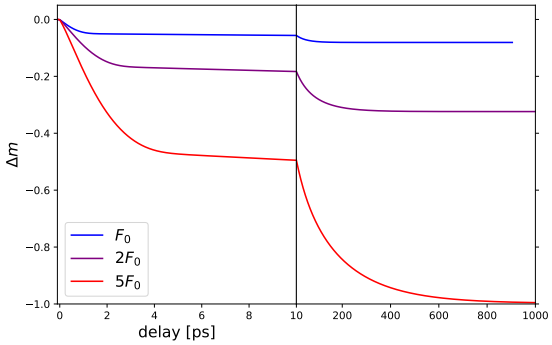

(a) Laser induced magnetization dynamics $\Delta m = m - m(t = 0)$ for three different fluences. Initial temperature $T_0 = 20$ K and $F_0 = 0.01$ mJ/cm^2.

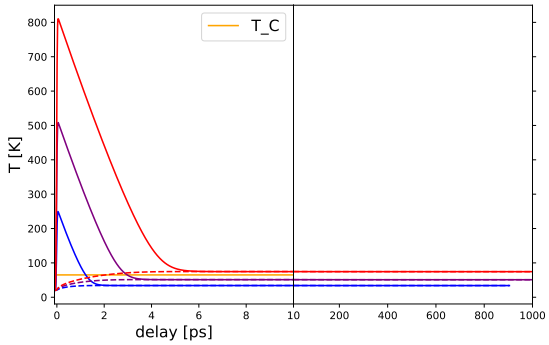

(b) Electron- and lattice temperature dynamics for three different fluences (see panel (a)). Initial temperature $T_0 = 20$ K and $F_0 = 0.01$ mJ/cm^2.

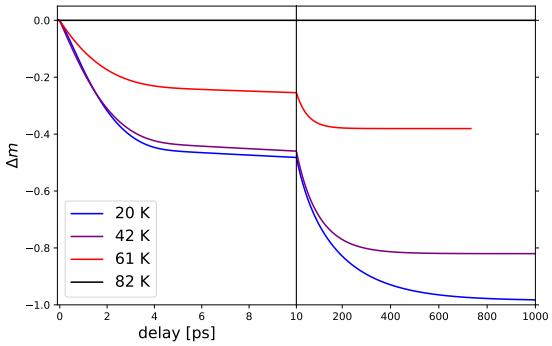

(a) Laser induced magnetization dynamics $\Delta m = m - m(t = 0)$ for four different initial temperatures for a fixed absorbed fluence value of $F = 5F_0 = 0.05$ mJ/cm^2.

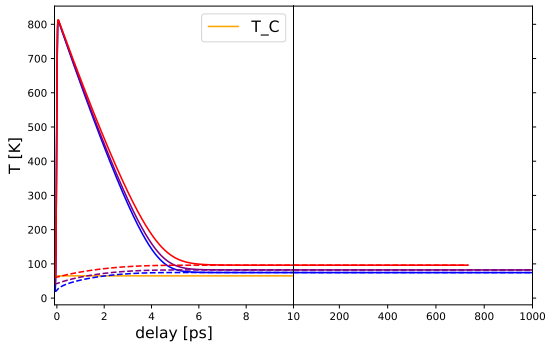

(b) Corresponding Electron- and lattice dynamics for absorbed fluence $F = 0.05$ $\frac{\text{mJ}}{\text{cm}^2}$ at different initial temperatures (see panel (a)).

* u.atxitia@csic.es

[1] M. Beens, M. L. M. Lalieu, A. J. M. Deenen, R. A. Duine, and B. Koopmans. Comparing all-optical switching in synthetic-ferrimagnetic multilayers and alloys. *Phys. Rev. B*, 100:220409, Dec 2019.

[2] B. Koopmans, G. Malinowski, F. Dalla Longa, D. Steiauf, M. Fähnle, T. Roth, M. Cinchetti, and M. Aeschlimann. Explaining the paradoxical diversity of ultrafast laser-induced demagnetization. *Nature Materials*, 9(3):259–265, 2010.

[3] S. Spachmann, A. Elghandour, S. Selter, B. Büchner, S. Aswartham, and R. Klingeler. Strong effects of uniaxial pressure and short-range correlations in cr2ge2te6. 02 2022.

[4] D. Zahn, F. Jakobs, Y. W. Windsor, H. Seiler, T. Vasileiadis, T. A. Butcher, Y. Qi, D. Engel, U. Atxitia, J. Vorberger, and R. Ernstorfer. Lattice dynamics and ultrafast energy flow between electrons, spins, and phonons in a 3d ferromagnet. *Phys. Rev. Research*, 3:023032, Apr 2021.